

Enhancing Neutrosophic Weibull-G Family: Simulation and Applications on Neutrosophic Data

Nooruldeen A. Noori^{1*}, Alaa A. Elnazer², Mundher A. Khaleel³, Mohammed Elgarhy^{4,5}, Ehab M. Almetwally⁶

¹ Anbar Education Directorate, Anbar, Iraq; Nooruldeen.a.noori35508@st.tu.edu.iq

² Department of Marketing, College of Business, Imam Mohammad Ibn Saud Islamic University (IMSIU), Riyadh 11432, Saudi Arabia; aaelnazer@imamu.edu.sa

³ Mathematics Departments, College of Computer Science and Mathematics, Tikrit University, Iraq; mun880088@tu.edu.iq

⁴ Department of Computer Engineering, Biruni University, 34010, Istanbul, Turkey; dr.moelgarhy@biruni.edu.tr

⁵ Department of Basic Sciences, Higher Institute of Administrative Sciences, Belbeis, AlSharkia, Egypt; dr.moelgarhy@gmail.com

⁶ Department of Mathematics and Statistics, College of Science, Imam Mohammad Ibn Saud Islamic University (IMSIU), Riyadh, Saudi Arabia; emalmetwally@imamu.edu.sa

*Corresponding Author: Nooruldeen.a.noori35508@st.tu.edu.iq

Citation: Noori, N. A., Elnazer, A. A., Khaleel, M. A., Elgarhy, M. & Almetwally, E. M. (2025). Enhancing Neutrosophic Weibull-G Family: Simulation and Applications on Neutrosophic Data, *Journal of Cultural Analysis and Social Change*, 10(4), 1899-1915. <https://doi.org/10.64753/jcasc.v10i4.3098>

Published: December 10, 2025

ABSTRACT

This paper, propose a new family of continuous probability distributions that combines the Weibull distribution and T-X method to generate the modified family and then combine it with Neutrosophic framework. This family is known as the Neutrosophic Modified Weibull-G (NMW-G) family. Also present the Neutrosophic Modified Weibull Exponential (NMW-E) distribution. The effectiveness of the NMW-E was tested on real neutrosophic data (time to failure of 20 electronic components) and compared with several neutrosophic distributions using specific statistical methods. Five simulations methods were also performed to estimate parameters using: MLE, LSE, WLSE, ADE, and RTADE, and their associated statistical properties were analyzed. The results demonstrated high accuracy and flexibility of the proposed distribution compared to other classical distributions.

Keywords: Neutrosophic distribution, Modified Weibull, uncertain data, Statistical Simulations, and parameter estimation

INTRODUCTION

In statistic and probability theory, continuous probability distributions are essential tools for modeling random phenomena that take values in a continuous space (such as physical measurements, time or any infinitely divisible quantities). These distributions are classified into families that differ in their mathematical properties and practical applications. They are expressed as a set of distributions that share a common mathematical formula but differ in values of the parameters that determine their shape and properties. Several families of statistical distributions have been presented, including: TG-G class [1], OCG family [2], NGOFE-G Family [3], and RTX-G family [4].

In the world of real-world data, information is often inaccurate, incomplete, or conflicting. This type of ambiguity cannot be accurately addressed using classical statistical tools. Here neutrosophic logic emerges as a powerful tool, allowing us to combine the element of "Truth-Falseness-Uncertainty" to form a more realistic view. To address these problems in data containing uncertainty, Florentin introduced the tools of neutrosophic logic to control this ambiguity [5], [6].

Despite these advancements, a significant gap remains: no existing neutrosophic distribution combines the flexibility of the Weibull distribution with the T-X transformation method while explicitly incorporating the

exponential distribution as a baseline. The Weibull distribution is renowned for its adaptability in modeling lifetime data, but its classical form cannot capture the inherent uncertainty in real-world datasets. Recent neutrosophic models, such as those in [7], [8], [9], [10], [11], [12], have addressed specific applications but lack the comprehensive mathematical structure and parameter estimation rigor required for broader applicability.

This study bridges this gap by introducing the Neutrosophic Modified Weibull-G (NMW-G) family, which generalizes the classical Weibull distribution within a neutrosophic framework. Our key contributions are:

- The NMW-G family is the first to integrate the Weibull distribution with the T-X method under neutrosophic logic, enabling the modeling of data with inherent ambiguity.
- Derive the full structure of the NMW-G family, including its neutrosophic cumulative distribution function (NCDF), probability density function (Npdf), survival and hazard functions, and quantile analysis.
- Demonstrate the superiority of the NMW-E (Exponential baseline) sub-model over existing neutrosophic distributions (e.g., NOL-E, NK-E, NB-E) using real-world failure time data, validated by statistical criteria (AIC, BIC) and goodness-of-fit tests.
- Employ five parameter estimation methods (MLE, LSE, WLSE, ADE, RTADE).

This work not only extends the theoretical foundations of neutrosophic statistics but also provides a practical tool for analyzing complex, uncertain datasets, outperforming recent models like the neutrosophic Beta-Lindley [11] and generalized Pareto [12] in flexibility and accuracy.

The research objective to present a family of neutrosophic distributions and a distribution derived from it that reflects the neutrosophic nature of data derive and analyze its mathematical properties, test it on real data, and compare the performance of different parameter estimation methods through simulation.

Neutrosophic Modified Weibull-G (NMW-G) Family

This family combines the classical Weibull distribution with neutrosophic framework to handle data of an ambiguous or uncertain nature. It was developed using the T-X method which introduced in 2014 by [13], to generate new distributions. The process begins with the classical Weibull distribution, whose cumulative density function (CDF) and probability density function (pdf) are given by:

$$Q(x) = 1 - e^{-rx^u} \tag{1}$$

$$q(x) = rux^{u-1}e^{-rx^u}, x \geq 0 \tag{2}$$

where r, u shape parameters for Weibull distribution.

The T-X transformation is then applied to CDF function $Q(x)$ of any underlying distribution to create a new family. The transformation used here is:

$$W(G) = \frac{(F(x))^2}{1 - F(x)} \tag{3}$$

This transformation enhances to flexibility of the new distribution in representing data with heavy tails or asymmetric shapes. Using the above transformation in equation (3), the CDF for the new family is defined as follows:

$$G(x) = \int_0^{W(G)} rux^{u-1}e^{-rx^u} dx = \int_0^{\frac{(F(x))^2}{1-F(x)}} rux^{u-1}e^{-rx^u} dx$$

$$G(x) = 1 - e^{-r\left(\frac{(F(x))^2}{1-F(x)}\right)^u} \tag{4}$$

Equation (4) is called the CDF function for Modified Weibull-G (MW-G) family, from this equation, the pdf is derived by differentiating $G(x)$ with respect to x to get a final form:

$$g(x) = rue^{-r\left(\frac{(F(x))^2}{1-F(x)}\right)^u} \left(\frac{(F(x))^2}{1-F(x)}\right)^{u-1} \frac{F(x)f(x)(2 - F(x))}{(1 - F(x))^2} \tag{5}$$

where $f(x)$ is the density function of the underlying distribution $F(x)$.

To represent uncertainty in the data, the parameters r and u are generalized to be neutrosophic (i.e., they contain a degree of ambiguity), and are written as r_N and u_N . The parameters and the variable x_N become neutrosophic. Thus, according to neutrosophic logic, the two functions become:

$$G(x_N) = 1 - e^{-r_N\left(\frac{(F(x_N))^2}{1-F(x_N)}\right)^{u_N}} \tag{6}$$

$$g(x_N) = r_N u_N e^{-r_N \left(\frac{(F(x_N))^2}{1-F(x_N)} \right)^{u_N}} \left(\frac{(F(x_N))^2}{1-F(x_N)} \right)^{u_N-1} \frac{F(x_N) f(x_N) (2-F(x_N))}{(1-F(x_N))^2} \tag{7}$$

Equation 6 the neutrosophic CDF (NCDF) and equation 7 the neutrosophic pdf (Npdf) of the Neutrosophic Modified Weibull-G (NMW-G) family. This mathematical structure allows for the analysis of data of uncertain nature, such as the "failure time" study of electronics mentioned in the paper, where the new distribution outperformed classical distributions.

Neutrosophic Modified Weibull- Exponential (NMW-E) Distribution

Using the Exponential distribution as a baseline, the CDF and pdf of Exponential are $F(x) = 1 - e^{-cx}$ and $f(x) = ce^{-cx}$, respectively. While the Neutrosophic CDF and pdf of Exponential are given by:

$$F(x_N) = 1 - e^{-c_N x_N} \tag{8}$$

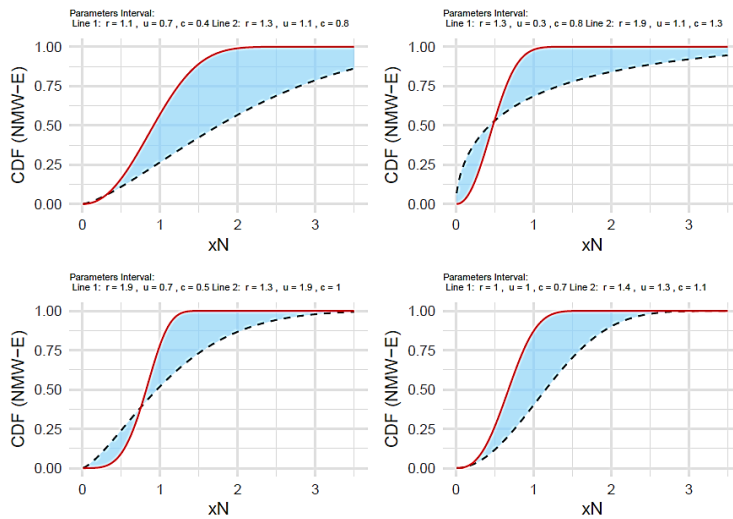
$$f(x) = c_N e^{-c_N x_N} \tag{9}$$

Substituting above equations into equations (6) and (7) yields the NCDF and Npdf of Neutrosophic Modified Weibull- Exponential (NMW-E) distribution to get a form:

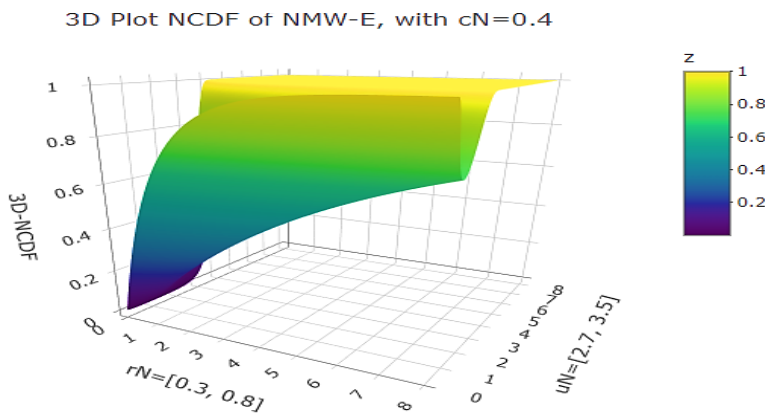
$$G(x_N) = 1 - e^{-r_N \left(\frac{(1-e^{-c_N x_N})^2}{e^{-c_N x_N}} \right)^{u_N}} \tag{10}$$

$$g(x) = r_N u_N c_N \frac{(1 - e^{-c_N x_N})^{2u_N-1} (1 + e^{-c_N x_N})}{e^{-u_N c_N x_N}} e^{-r_N \left(\frac{(1-e^{-c_N x_N})^2}{e^{-c_N x_N}} \right)^{u_N}} \tag{11}$$

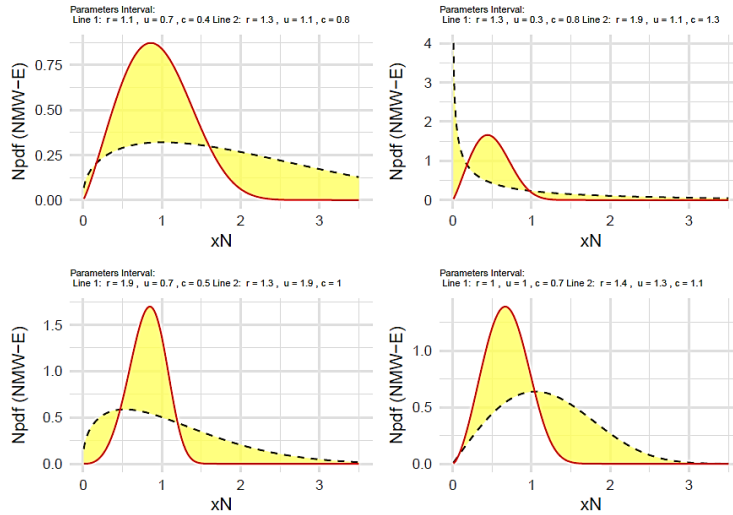
To verify the nature of NMW-E distribution and its flexibility in different data, the basic distribution functions are plotted. Figures 1 to 4 represent the plot of NCDF function, 3D plot of NCDF, Npdf function, and 3D plot of Npdf, respectively.



Figures 1. plot of NCDF function for NMW-E distribution

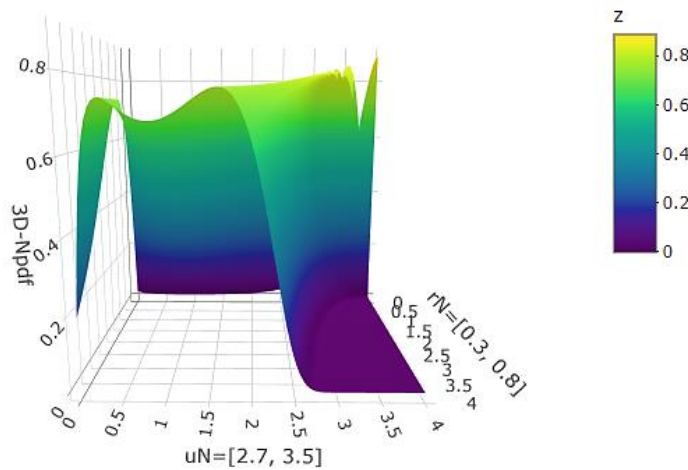


Figures 2. 3D-plot of NCDF function for NMW-E distribution



Figures 3. plot of Npdf function for NMW-E distribution

3D Plot Npdf of NMW-E, with $c_N=0.4$



Figures 4. 3D-plot of Npdf function for NMW-E distribution

Figure 1 shows the modified cumulative distribution function (CDF) for the new NMW-E distribution. It illustrates how probabilities gradually accumulate as the value of the neutrosophic random variable x_N increases. If the curve starts from zero (when $x_N = 0$) and approaches 1 (when $x_N \rightarrow \infty$), this indicates that the function obeys the properties of a traditional CDF but in a modified form. It exhibits nonlinear behavior (such as concavity or kurtosis) that reflects the characteristics of the new distribution, such as flexibility in the accumulation pattern due to the additional parameters. Figure 2 shows the relationship between the cumulative distribution function (NCDF) and the two new parameters and how the shape of the CDF changes when the distribution parameters are modified.

Figure 3 shows the probability density function (PDF) for the new distribution. The shape of the distribution (such as exponential, polar, or polypeak) represents a single peak (unimodal), demonstrating the flexibility of the distribution in modeling diverse data. Compared to the traditional Weibull, you may see improvements such as greater flexibility in representing extreme data. Figure 4 This 3D plot shows the relationship of the NPDF to two parameters. How the shape of the PDF changes (such as peak regularity or tail spreading) when the parameters are changed.

Some Statistical Properties of NMW-E Distribution

This section presents some statistical properties of NMW-E distribution, which are as follows:

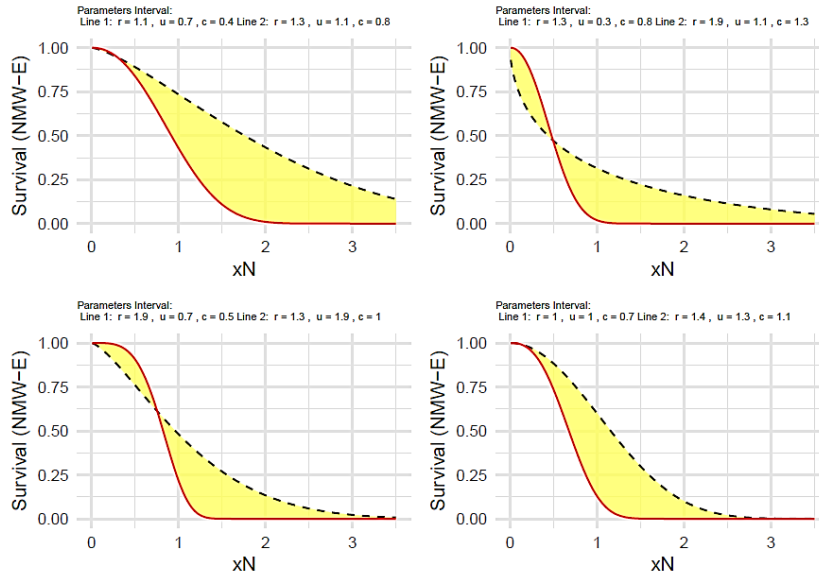
Survival and Hazard Functions of NMW-E Distribution

The Survival function of NMW-E distribution can be derived from form:

$$S(x_N) = 1 - G(x_N)$$

$$G(x_N) = 1 - e^{-r_N \left(\frac{(1 - e^{-c_N x_N})^2}{e^{-c_N x_N}} \right)^{u_N}} \tag{12}$$

Figures 5 represent the plot of Survival function.



Figures 5. plot of Survival function for NMW-E distribution

The difference in parameter values between scenarios indicates that different conditions were tested to assess their impact on survival. For example, if r_N is higher and u_N is lower, this indicates favorable conditions for survival, while the opposite indicates more difficult conditions.

While the Hazard function of NMW-E distribution can be derived from form:

$$h(x_N) = \frac{g(x_N)}{S(x_N)}$$

$$h(x_N) = r_N u_N c_N \frac{(1 - e^{-c_N x_N})^{2u_N - 1} (1 + e^{-c_N x_N})}{e^{-u_N c_N x_N}} \tag{13}$$

Expansion NCDF and Npdf of NMW-E Distribution

Given the difficulty of dealing with basic distribution functions in equations 10 and 11 in finding statistical properties, Taylor and binomial series have been used to expand NCDF and Npdf of NMW-E distribution, facilitating their analysis and calculating of their statistical properties. These expansions allow the functions to be represented as infinite series that can be approximated numerically. Then we have get NCDF by using the expansion of the exponential function:

$$e^{-r_N \left(\frac{(1 - e^{-c_N x_N})^2}{e^{-c_N x_N}} \right)^{u_N}} = \sum_{i_N=0}^{\infty} \frac{(-1)^{i_N}}{i_N!} r_N^{i_N} \frac{(1 - e^{-c_N x_N})^{2(i_N u_N)}}{e^{-c_N i_N u_N x_N}}$$

Using the binomial series expansion for $(1 - e^{-c_N x_N})^{2(i_N u_N)}$ to get:

$$(1 - e^{-c_N x_N})^{2i_N u_N} = \sum_{j_N=0}^{\infty} (-1)^{j_N} \binom{2(i_N u_N)}{j_N} e^{-j_N c_N x_N}$$

Hence

$$e^{-r_N \left(\frac{(1 - e^{-c_N x_N})^2}{e^{-c_N x_N}} \right)^{u_N}} = \sum_{i_N=j_N=0}^{\infty} \frac{(-1)^{i_N+j_N}}{i_N!} \binom{2(i_N u_N)}{j_N} r_N^{i_N} \frac{e^{-j_N c_N x_N}}{e^{-c_N i_N u_N x_N}}$$

$$e^{-r_N \left(\frac{(1 - e^{-c_N x_N})^2}{e^{-c_N x_N}} \right)^{u_N}} = \sum_{i_N=j_N=0}^{\infty} \frac{(-1)^{i_N+j_N}}{i_N!} \binom{2(i_N u_N)}{j_N} r_N^{i_N} e^{-c_N x_N (j_N - i_N u_N)}$$

To get a final form:

$$G(x_N) = 1 - \text{He}^{-c_N x_N (j_N - i_N u_N)} \tag{14}$$

where $H = \sum_{i_N=j_N=0}^{\infty} \frac{(-1)^{i_N+j_N}}{i_N!} \binom{2i_N u_N}{j_N} r_N^{i_N}$

and Npdf by form:

$$g(x) = \psi(e^{-c_N x_N(p_N+u_N(i_N+1))} + e^{-c_N x_N(p_N-u_N(i_N+1)+1)}) \tag{15}$$

where $\psi = \sum_{i_N=p_N=0}^{\infty} \frac{(-1)^{i_N+p_N}}{i_N!} \binom{2(i_N u_N)+2u_N-1}{p_N} r_N^{i_N+1} u_N c_N$

while the $NCDF^{\beta_N}$ have a form:

$$G^{\beta_N}(x_N) = \left(1 - e^{-r_N \left(\frac{(1-e^{-c_N x_N})^2}{e^{-c_N x_N}} \right)^{u_N}} \right)^{\beta_N} \tag{16}$$

And can be expansion by form:

$$G^{\beta_N}(x_N) = \varphi e^{-c_N x_N(s_N-u_N k_N)} \tag{17}$$

where $\varphi = \sum_{i_N=s_N=k_N=0}^{\infty} \frac{(-1)^{i_N+s_N+k_N}}{k_N!} \binom{\beta_N}{i_N} \binom{2(u_N k_N)}{s_N} r_N^{k_N} i_N^{k_N}$

The Moment of NMW-E Distribution

Let x_N be an arbitrary neutrosophic random variable with a Npdf by equation 16. The n^{th} neutrosophic moment of NMW-E distribution is represented as follows [14]:

$$\mu_n = E(x^n) = \int_0^{\infty} x^n g(x_N) dx_N$$

$$\mu_n = \psi \int_0^{\infty} x^n (e^{-c_N x_N(p_N+u_N(i_N+1))} + e^{-c_N x_N(p_N-u_N(i_N+1)+1)}) dx_N$$

$$\mu_n = \psi(I_1 dx_N + I_2 dx_N)$$

where $I_1 = \int_0^{\infty} x^n e^{-c_N x_N(p_N+u_N(i_N+1))} dx_N$ and $I_2 = \int_0^{\infty} x^n e^{-c_N x_N(p_N-u_N(i_N+1)+1)} dx_N$

For I_1 , let $y = c_N x_N(p_N + u_N(i_N + 1))$

$$x_N = \frac{y}{c_N(p_N + u_N(i_N + 1))} \Rightarrow dx_N = \frac{1}{c_N(p_N + u_N(i_N + 1))} dy$$

$$\text{Then } I_1 = \int_0^{\infty} \left(\frac{y}{c_N(p_N+u_N(i_N+1))} \right)^n e^{-y} \frac{1}{c_N(p_N+u_N(i_N+1))} dy$$

Simplify I_1 to achieve the following final form :

$$I_1 = \frac{1}{(c_N(p_N + u_N(i_N + 1)))^n c_N(p_N + u_N(i_N + 1))} \int_0^{\infty} y^n e^{-y} dy$$

$$I_1 = \frac{1}{(c_N(p_N + u_N(i_N + 1)))^n c_N(p_N + u_N(i_N + 1))} \Gamma(n + 1)$$

For I_2 let $u = c_N x_N(p_N - u_N(i_N + 1) + 1)$

$$x_N = \frac{u}{c_N(p_N - u_N(i_N + 1) + 1)} \Rightarrow dx_N = \frac{1}{c_N(p_N - u_N(i_N + 1) + 1)} du$$

$$I_2 = \int_0^{\infty} \left(\frac{u}{c_N(p_N - u_N(i_N + 1) + 1)} \right)^n e^{-u} \frac{1}{c_N(p_N - u_N(i_N + 1) + 1)} du$$

$$I_2 = \frac{1}{(c_N(p_N - u_N(i_N + 1) + 1))^n c_N(p_N - u_N(i_N + 1) + 1)} \int_0^{\infty} u^n e^{-u} du$$

$$I_2 = \frac{1}{(c_N(p_N - u_N(i_N + 1) + 1))^n c_N(p_N - u_N(i_N + 1) + 1)} \Gamma(n + 1)$$

Then the final form for μ_n :

$$\mu_n = \psi \Gamma(n + 1) \left[\frac{1}{(c_N(p_N + u_N(i_N + 1)))^{n+1}} + \frac{1}{(c_N(p_N - u_N(i_N + 1) + 1))^{n+1}} \right] \tag{18}$$

The initial four neutrosophic moment are determined by inserting the value of n as follows:

$$\mu_1 = \psi \left[\frac{1}{(c_N(p_N + u_N(i_N + 1)))^2} + \frac{1}{(c_N(p_N - u_N(i_N + 1) + 1))^2} \right] \tag{19}$$

$$\mu_2 = 2\psi \left[\frac{1}{(c_N(p_N + u_N(i_N + 1)))^3} + \frac{1}{(c_N(p_N - u_N(i_N + 1) + 1))^3} \right] \tag{20}$$

$$\mu_3 = 6\psi \left[\frac{1}{(c_N(p_N + u_N(i_N + 1)))^4} + \frac{1}{(c_N(p_N - u_N(i_N + 1) + 1))^4} \right] \tag{21}$$

$$\mu_4 = 24\psi \left[\frac{1}{(c_N(p_N + u_N(i_N + 1)))^5} + \frac{1}{(c_N(p_N - u_N(i_N + 1) + 1))^5} \right] \tag{22}$$

The neutrosophic skewness and neutrosophic kurtosis of the NMW-E distribution as follows [15]:

$$SK_N = \frac{6\psi \left[\frac{1}{(c_N(p_N + u_N(i_N + 1)))^4} + \frac{1}{(c_N(p_N - u_N(i_N + 1) + 1))^4} \right]}{\left(2\psi \left[\frac{1}{(c_N(p_N + u_N(i_N + 1)))^3} + \frac{1}{(c_N(p_N - u_N(i_N + 1) + 1))^3} \right] \right)^{\frac{3}{2}}} \tag{23}$$

$$KU_N = \frac{6\psi \left[\frac{1}{(c_N(p_N + u_N(i_N + 1)))^5} + \frac{1}{(c_N(p_N - u_N(i_N + 1) + 1))^5} \right]}{\left(\psi \left[\frac{1}{(c_N(p_N + u_N(i_N + 1)))^3} + \frac{1}{(c_N(p_N - u_N(i_N + 1) + 1))^3} \right] \right)^2} - 3 \tag{24}$$

Table 1 represents an analysis of some moments of NMW-E distribution. the first four statistical moments, variance, skewness and kurtosis were calculated for different periods of the parameters, allowing for understanding the distributions behavior under carrying conditions.

Table.1 some intervals of moments for NMW-E distribution

r_N	u_N	c_N	μ_1	μ_2	μ_3	μ_4	σ_N^2	SK_N	KU_N
[0.5,1.5]	[0.4,1.4]	[0.1,1.1]	[0.033363, 0.560671]	[0.021304, 0.390407]	[0.015639, 0.291334]	[0.012351, 0.228287]	[0.020191, 0.076055]	[5.029229, 1.194304]	[27.21193, 1.497771]
		[0.2,1.2]	[0.055879, 0.564378]	[0.035512, 0.376236]	[0.025999, 0.270471]	[0.020498, 0.205261]	[0.03239, 0.057713]	[3.884987, 1.17201]	[16.25385, 1.450059]
	[0.6,1.6]	[0.3,1.3]	[0.059967, 0.574051]	[0.040878, 0.36803]	[0.03098, 0.252966]	[0.024932, 0.183316]	[0.037282, 0.038496]	[3.74842, 1.133018]	[14.92016, 1.353422]
		[0.4,1.4]	[0.082466, 0.54234]	[0.056034, 0.326236]	[0.042382, 0.211074]	[0.034062, 0.144474]	[0.049234, 0.032103]	[3.195226, 1.132754]	[10.84821, 1.357453]
[0.7,1.7]	[0.7,1.7]	[0.5,1.5]	[0.13341, 0.497249]	[0.092475, 0.271177]	[0.070615, 0.158415]	[0.057061, 0.097718]	[0.074677, 0.023921]	[2.511097, 1.121803]	[6.672517, 1.328834]
		[0.6,1.6]	[0.165342, 0.466259]	[0.114015, 0.238424]	[0.086767, 0.130611]	[0.069945, 0.075562]	[0.086677, 0.021026]	[2.253804, 1.121902]	[5.380634, 1.329255]

	[0.9,1.9]	[0.7,1.7]	[0.19737, 0.448775]	[0.142275, 0.217325]	[0.110917, 0.111536]	[0.090757, 0.05998]	[0.10332, 0.015926]	[2.06683, 1.100911]	[4.48356, 1.269966]
	[0.8,1.8]		[0.238933, 0.423843]	[0.171131, 0.193848]	[0.132805, 0.09396]	[0.108298, 0.047722]	[0.114041, 0.014206]	[1.875956, 1.100911]	[3.697989, 1.269965]

From above table $\hat{\mu}_{1N}$ (the mean) represents the neutrosophic expected value of NMW-E distribution. note that : as c_N increases, the $\hat{\mu}_{1N}$ decreases (e.g. at $c_N = [0.1,1.1]$ become $\hat{\mu}_{1N} = [0.033,0.560]$, while at $c_N = [0.8,1.8]$ become $\hat{\mu}_{1N} = [0.238,0.423]$). increasing r_N implies increases $\hat{\mu}_{1N}$ compare rows with $r_N = [0.5,1.5]$ with $r_N = [0.7,1.7]$. $\hat{\mu}_{2N}, \hat{\mu}_{3N}$, and $\hat{\mu}_{4N}$ which are used to calculate neutrosophic variance, neutrosophic skewness, and neutrosophic kurtosis. Neutrosophic variance refers to the degree of dispersion of data around neutrosophic mean, observe that the neutrosophic variance decreases as c_N increases at $c_N = [0.1,1.1]$ become $\sigma_N^2 = [0.020,0.076]$, while when $c_N = [0.8,1.8]$ become $\sigma_N^2 = [0.114,0.014]$, as u_N increases, σ_N^2 decreases, indicating that the data is concentrated around neutrosophic mean. The coefficient of skewness measures the degree of asymmetry of the distribution. Positive values indicate a right-skewed distribution. We observe that it decreases as c_N increases. A decrease in u_N indicates that the distribution is approaching symmetry.

The neutrosophic moments generating function (Nmgf) for NMW-E distribution can be founded using moment equation 18 and exponential expansion [16] to get from:

$$M_x(t) = \sum_{r=0}^{\infty} \frac{t^r}{r!} \left[\psi \Gamma(n+1) \left[\frac{1}{(c_N(p_N+u_N(i_N+1)))^{n+1}} + \frac{1}{(c_N(p_N-u_N(i_N+1)+1))^{n+1}} \right] \right] \tag{25}$$

The neutrosophic Characteristic function for NMW-E distribution can be founded using neutrosophic moment equation 18 and exponential expansion to get from:

$$Q_x(t) = \sum_{v=0}^{\infty} \frac{(it)^v}{v!} \left[\psi \Gamma(n+1) \left[\frac{1}{(\mathcal{E}c_N)^{n+1}} + \frac{1}{(c_N(p_N-u_N(i_N+1)+1))^{n+1}} \right] \right] \tag{26}$$

Neutrosophic Incomplete Moments

Let x_N be an arbitrary neutrosophic random variable with a Npdf by equation 16. The n^{th} neutrosophic incomplete moment of NMW-E distribution is represented as follows:

$$M_n(y) = \int_{-\infty}^y x^n g(x) dx_N$$

By same way in prove moments we can get a final form:

$$M_n(y) = \psi \left[\frac{\Gamma((n+1), \mathcal{E}c_N y)}{(\mathcal{E}c_N)^{n+1}} + \frac{\Gamma((n+1), c_N y(p_N - u_N(i_N + 1) + 1))}{(c_N y(p_N - u_N(i_N + 1) + 1))^{n+1}} \right] \tag{27}$$

where $\mathcal{E} = p_N + u_N(i_N + 1)$

The Neutrosophic Quantile Function

The neutrosophic quantile function $Q_N(q_N)$ is derived from the equation [17]: $Q_N(q_N) = G^{-1}(x_N)$, where $Q_N(q_N)$ represent the neutrosophic quantile function for NMW-E distribution for each q_N in the range (0,1). Take

$$q_N = G(x_N)$$

Then using some mathematical operation, we get a final form:

$$Q_N(q_N) = \frac{-\log(A)}{c_N} \tag{28}$$

$$\text{where } A = \frac{\left(\left(\frac{-\log(1-q_N)}{r_N} \right)^{\frac{1}{u_N} + 1} \right) \mp \sqrt{\left(\left(\frac{-\log(1-q_N)}{r_N} \right)^{\frac{1}{u_N} + 1} \right)^{\frac{2}{u_N}} + 4}}{2}$$

Table 2 shows the quantile values (percentages) such as (0.1, 0.2, ..., 0.9) for different sets of parameters (r_N, u_N, c_N). These values are used in determining critical thresholds for predicting failure or endurance in

engineering applications, reliability analysis of confidence intervals under uncertainties, and comparison of distributions when changing parameters.

Table 2: Quintile function for NMW-E distribution

q_N	(r_N, u_N, c_N)				
	$[0.3, 1.3], [0.6, 1.6]$ $[0.8, 1.8]$	$[0.9, 1.9], [0.5, 1.5]$ $[0.6, 1.6]$	$[0.8, 1.8], [0.6, 1.6]$ $[0.4, 1.4]$	$[0.9, 1.9], [0.6, 1.6]$ $[0.7, 1.7]$	$[0.5, 1.5], [0.7, 1.7]$ $[1, 2]$
0.1	[0.5188950, 0.2511940]	[0.1949995, 0.2369119]	[0.4609341, 0.2921734]	[0.2388252, 0.2366430]	[0.3273285, 0.2269761]
0.2	[0.9534936, 0.3160006]	[0.4121778, 0.3030933]	[0.8584608, 0.3679071]	[0.4450795, 0.2980158]	[0.5548398, 0.2817588]
0.3	[1.3737165, 0.3642970]	[0.6562614, 0.3531536]	[1.2618150, 0.4244327]	[0.6548386, 0.3438426]	[0.7667080, 0.3221141]
0.4	[1.7906727, 0.4058279]	[0.9337149, 0.3966885]	[1.6880047, 0.4731778]	[0.8772607, 0.3833680]	[0.9761929, 0.3566111]
0.5	[2.2118162, 0.4444836]	[1.2538290, 0.4375920]	[2.1514613, 0.5186091]	[1.1202544, 0.4202441]	[1.1910838, 0.3885838]
0.6	[2.6467216, 0.4827060]	[1.6309690, 0.4783492]	[2.6705692, 0.5636716]	[1.3941073, 0.4568078]	[1.4192134, 0.4200627]
0.7	[3.1115421, 0.5228553]	[2.0899357, 0.5215787]	[3.2752871, 0.6111033]	[1.7156225, 0.4952896]	[1.6717150, 0.4530341]
0.8	[3.6395071, 0.5687443]	[2.6816724, 0.5712712]	[4.0267573, 0.6654082]	[2.1190959, 0.5393952]	[1.9703239, 0.4905476]
0.9	[4.3256376, 0.6299274]	[3.5523934, 0.6382464]	[5.1010691, 0.7381396]	[2.7033898, 0.5985145]	[2.3766167, 0.5404588]

Table 2 shows the sensitivity of NMW-E distribution to parameters. NMW-E distribution reacts strongly to change in r_N and c_N , while showing relative stability with u_N . The high values at neutrosophic quantiles of 0.8 and 0.9 indicate right tail, typical of distributions used in stress tolerance.

Meaning that increasing r_N leads to an increase in the range and upper values, while increasing c_N leads to a general decrease in the values. As for increasing u_N it leads to narrowing the intervals (reducing the variance). This analysis demonstrates the flexibility of values the NMW-E distribution in representing data under uncertainty, making it suitable for complex applications such as Stress – Strength reliability.

3.1 Stress – Strength reliability

It's an important statistical measure in reliability analysis and engineering. It measures the probability that the strength of system or component will be greater than the applied stress. Mathematically, this property is given by relationship:

$$R = P(X_2 < X_1) = \int_0^\infty g_{X_1}(r_N, u_N, c_N) G_{X_2}(r_{2N}, u_{2N}, c_{2N}) dx_N$$

Using equations 10 and 11 we arrive at

$$G_{X_2}(r_{2N}, u_{2N}, c_{2N}) = 1 - e^{-r_{2N} \left(\frac{(1 - e^{-c_{2N}x_N})^2}{e^{-c_{2N}x_N}} \right)^{u_{2N}}}$$

Using the expansion of the exponential function

$$e^{-r_{2N} \left(\frac{(1 - e^{-c_{2N}x_N})^2}{e^{-c_{2N}x_N}} \right)^{u_{2N}}} = \sum_{i_N=0}^\infty \frac{(-1)^{i_N}}{i_N!} r_{2N}^{i_N} \frac{(1 - e^{-c_{2N}x_N})^{2(i_N u_{2N})}}{e^{-c_{2N}i_N u_{2N} x_N}}$$

Using the binomial series expansion

$$(1 - e^{-c_{2N}x_N})^{2(i_N u_{2N})} = \sum_{j_N=0}^\infty (-1)^{j_N} \binom{2(i_N u_{2N})}{j_N} e^{-j_N c_{2N} x_N}$$

Continuously by same way to get a final form:

$$G_{X_2}(r_{2N}, u_{2N}, c_{2N}) = 1 - \psi e^{-c_{2N}x_N(j_N - i_N u_{2N})}$$

where $H = \sum_{i_N=j_N=0}^\infty \frac{(-1)^{i_N+j_N}}{i_N!} \binom{2(i_N u_{2N})}{j_N} r_{2N}^{i_N}$, then we get:

$$R = \int_0^\infty g_{X_1}(r_N, u_N, c_N) [1 - \psi e^{-c_{2N}x_N(j_N - i_N u_{2N})}] dx_N$$

$$R = \int_0^\infty g_{X_1}(r_N, u_N, c_N) dx_N - \int_0^\infty [1 - \psi e^{-c_{2N}x_N(j_N - i_N u_{2N})}] g_{X_1}(r_N, u_N, c_N) dx_N$$

Since $\int_0^\infty g_{X_1}(r_N, u_N, c_N) dx_N = 1$, hence we get:

$$R = 1 - \int_0^\infty [1 - \psi e^{-c_{2N}x_N(j_N - i_N u_{2N})}] g_{X_1}(r_N, u_N, c_N) dx_N \tag{29}$$

3.2 Entropy Rényi

The Entropy Rényi for NMW-E distribution can be founded using formula [18]:

$$I_R(p) = \frac{1}{1-p} \log \int_0^\infty g(x_N)^p dx_N$$

Then the final form for Entropy Rényi for NMW-E distribution is:

$$I_R(p) = \frac{1}{1-p} \log \left[\sum_{k_N=0}^p (-1)^{k_N} \binom{p}{k_N} \psi^p \frac{1}{c_N(p_N p + u_N(i_N+1)p + k_N(1-2u_N(i_N+1)))} \right] \tag{30}$$

Estimation

Maximum Likelihood Estimation

The maximum likelihood estimation approach is used to calculate the parameters of NMW-E distribution. for random sample of data points $x_{N1}, x_{N2}, \dots, x_{Nn}$, we compute the log-likelihood function. the Npdf of distribution is identical to that of the NMW-E distribution [19]:

$$L(\Theta, x) = \prod_{i=1}^n g(x_{Ni})$$

$$L(\Theta, x) = \prod_{i=1}^n r_N u_N c_N \frac{(1 - e^{-c_N x_{Ni}})^{2u_N - 1} (1 + e^{-c_N x_{Ni}})}{e^{-u_N c_N x_{Ni}}} e^{-r_N \left(\frac{(1 - e^{-c_N x_{Ni}})^2}{e^{-c_N x_{Ni}}} \right)^{u_N}}$$

we compute the log- likelihood:

$$L = n \log(r_N) + n \log(u_N) + n \log(c) + (2u_N - 1) \sum_{i=1}^n (1 - e^{-c_N x_{Ni}})$$

$$+ \sum_{i=1}^n (1 + e^{-c_N x_{Ni}}) + u_N c_N \sum_{i=1}^n x_{Ni} - r_N \sum_{i=1}^n \left(\frac{(1 - e^{-c_N x_{Ni}})^2}{e^{-c_N x_{Ni}}} \right)^{u_N} \tag{31}$$

Least Square Estimation

The following equation can be used to estimate the parameters using Least square estimation (LSE) method:

$$\varphi(\theta_N) = \sum_{i=1}^m \left[G(x_{Ni}) - \frac{i}{n+1} \right]^2$$

$$\varphi(\theta_N) = \sum_{i=1}^n \left[1 - e^{-r_N \left(\frac{(1 - e^{-c_N x_{Ni}})^2}{e^{-c_N x_{Ni}}} \right)^{u_N}} - \frac{i}{n+1} \right]^2 \tag{32}$$

Weighted Least Square Estimation

The following equation can be used to estimate the parameters using Weighted Least square estimation (WLSE) method:

$$W(\theta_N) = \sum_{i=1}^n W_i \left[G(x_{Ni}) - \frac{i}{n+1} \right]^2$$

$$W(\theta_N) = \sum_{i=1}^n W_i \left[1 - e^{-r_N \left(\frac{(1 - e^{-c_N x_{Ni}})^2}{e^{-c_N x_{Ni}}} \right)^{u_N}} - \frac{i}{n+1} \right]^2 \tag{33}$$

In the three parts (4.1, 4.2, 4.3) of the parameters estimation section, equations 30 to 32 are partially derived with respect to the NMW-E distribution parameters and then this derivatives is set equal to zero to obtain an estimate of the parameters for three methods.

Statistical Simulations

Five techniques were used to evaluate the performed of the NMW-E distribution estimations: MLE, LSE, WLSE, ADE, and RTADE. The R programming language was used to implement these techniques in a Monte Carlo simulation. 1000 samples were selected for the simulation using actual parameter values listed in table 3, with sample sizes of 50, 100, 150, and 200. The estimated model parameters were averaged to calculate the mean values of the estimators, bias, mean squared error (MSE), and root mean squared error (RMSE) were than calculated.

Table.3: Monte Carlo simulations conducted for NMW-E distribution

$r_N = [3 , 4]$, $u_N = [1.5 , 1.9]$, $c_N = [4 , 5]$							
N	Est.	Ess. Par.	MLE	LSE	WLSE	ADE	RTADE
50	Mean	\hat{r}_N	[3.9917893, 5.143415]	[4.738623, 5.707372]	[4.328175, 5.373994]	[4.439933, 5.586339]	[13.66783, 16.72482]
		\hat{u}_N	[1.48804362, 1.96946326]	[0.6342964, 0.9787356]	[0.9317916, 1.2897713]	[1.0576053, 1.4499344]	[-19.71914, -24.13027]

	MSE	\widehat{c}_N	[4.1572593, 5.1066804]	[4.03414323, 4.8, 707255]	[4.03280694, 4.90882874]	[4.1392705, 5.04556834]	[0.4770653, 0.6105288]	
		\widehat{r}_N	[11.7349440, 20.590970]	[36.820765, 42.360068]	[22.351758, 31.253529]	[21.257898, 32.830854]	[156.29793, 213.87533]	
		\widehat{u}_N	[0.91061798, 1.61547104]	[5.3305295, 5.9705607]	[2.4585748, 3.6179930]	[2.1103319, 3.1313901]	[538.68577, 785.70433]	
	RMSE	\widehat{c}_N	[1.3654623, 1.7436138]	[2.28251487, 2.9297338]	[1.87948845, 2.39856760]	[1.7628712, 2.21794708]	[12.4434642, 19.3260501]	
		\widehat{r}_N	[3.4256305, 4.537727]	[6.068012, 6.508461]	[4.727765, 5.590486]	[4.610629, 5.729821]	[12.50192, 14.62448]	
		\widehat{u}_N	[0.95426306, 1.27101182]	[2.3087939, 2.4434731]	[1.5679843, 1.9021022]	[1.4526982, 1.7695734]	[23.20961, 28.03042]	
	Bias	\widehat{c}_N	[1.1685300, 1.3204597]	[1.51079941, 1.7116465]	[1.37094436, 1.54873097]	[1.3277316, 1.48927737]	[3.5275295, 4.3961404]	
		\widehat{r}_N	[0.9917893, 1.143415]	[1.738623, 1.707372]	[1.328175, 1.373994]	[1.439933, 1.586339]	[10.66783, 12.72482]	
		\widehat{u}_N	[0.01195638, 0.06946326]	[0.8657036, 0.9212644]	[0.5682084, 0.6102287]	[0.4423947, 0.4500656]	[21.21914, 26.03027]	
	100	Mean	\widehat{c}_N	[0.1572593, 0.1066804]	[0.03414323, 0.1292745]	[0.03280694, 0.09117126]	[0.1392705, 0.04556834]	[3.5229347, 4.3894712]
			\widehat{r}_N	[3.3371217, 4.5925015]	[3.5789559, 4.8551058]	[3.4446231, 4.7344332]	[3.5099832, 4.8252873]	[14.01895, 17.32226]
			\widehat{u}_N	[1.51818277, 1.91500837]	[1.1506284, 1.4378564]	[1.2995323, 1.608203]	[1.3361653, 1.6528578]	[-20.22584, -24.99249]
MSE		\widehat{c}_N	[4.02112953, 5.06446168]	[3.92451635, 4.90217145]	[3.96565557, 4.97987068]	[4.01959377, 5.04276528]	[0.4287158, 0.5636387]	
		\widehat{r}_N	[3.6125607, 7.3270065]	[8.4291834, 16.4321908]	[5.6892027, 11.5266142]	[5.4656765, 10.9631504]	[150.43933, 207.42677]	
		\widehat{u}_N	[0.35229733, 0.70861960]	[1.2640953, 2.1786850]	[0.70861960, 1.249400]	[0.6277198, 1.1773632]	[532.42010, 785.54847]	
RMSE		\widehat{c}_N	[0.62821559, 0.91991102]	[1.15557313, 1.68417783]	[0.82940438, 1.25063673]	[0.76376007, 1.17656029]	[12.7704225, 19.7189451]	
		\widehat{r}_N	[1.9006738, 2.7068444]	[2.9033056, 4.0536639]	[2.3852050, 3.3950868]	[2.3378786, 3.3110648]	[12.26537, 14.40232]	
		\widehat{u}_N	[0.59354640, 0.84179546]	[1.1243199, 1.4760369]	[0.8239700, 1.117766]	[0.7922877, 1.0850637]	[23.07423, 28.02764]	
Bias		\widehat{c}_N	[0.79260052, 0.95911992]	[1.07497588, 1.29775877]	[0.91071641, 1.11831871]	[0.87393367, 1.08469364]	[3.5735728, 4.4406019]	
		\widehat{r}_N	[0.3371217, 0.5925015]	[0.5789559, 0.8551058]	[0.4446231, 0.7344332]	[0.5099832, 0.8252873]	[11.01895, 13.32226]	
		\widehat{u}_N	[0.01818277, 0.01500837]	[0.3493716, 0.4621436]	[0.2004677, 0.291797]	[0.1638347, 0.2471422]	[21.72584, 26.89249]	
150	Mean	\widehat{c}_N	[0.02112953, 0.06446168]	[0.07548365, 0.09782855]	[0.03434443, 0.02012932]	[0.01959377, 0.04276528]	[3.5712842, 4.4363613]	
		\widehat{r}_N	[3.2330815, 4.3825372]	[3.5090559, 4.522526]	[3.3452902, 4.4250597]	[3.3715099, 4.4821055]	[14.25986, 18.02245]	
		\widehat{u}_N	[1.51730916, 1.92175581]	[1.2300223, 1.6148214]	[1.3665041, 1.7516043]	[1.3858205, 1.7765209]	[-20.57370, -26.00290]	
	MSE	\widehat{c}_N	[4.02293709, 5.05377072]	[3.992741011, 4.92003202]	[4.005035421, 4.98370275]	[4.02867704, 5.02388901]	[0.4154863, 0.5407019]	
		\widehat{r}_N	[2.2530450, 4.2097783]	[5.7130047, 9.617191]	[3.4001204, 6.2313956]	[3.2735087, 5.9360876]	[144.75355, 205.89467]	
		\widehat{u}_N	[0.22752012, 0.38801520]	[0.7809542, 1.2037000]	[0.3974947, 0.6700489]	[0.3939752, 0.6270253]	[524.65840, 797.86398]	
	RMSE	\widehat{c}_N	[0.41647403, 0.61431219]	[0.802778843, 1.20738948]	[0.557719932, 0.83127037]	[0.52553410, 0.78372013]	[12.8601771, 19.9116158]	
		\widehat{r}_N	[1.5010147, 2.0517744]	[2.3901893, 3.101160]	[1.8439415, 2.4962764]	[1.8092840, 2.4364087]	[12.03136, 14.34903]	
		\widehat{u}_N	[0.47699069, 0.62290866]	[0.8837161, 1.0971326]	[0.6304718, 0.8185651]	[0.6276745, 0.7918493]	[22.90542, 28.24649]	
	Bias	\widehat{c}_N	[0.64534799, 0.78378070]	[0.895979265, 1.09881276]	[0.746806489, 0.91174030]	[0.72493731, 0.88527969]	[3.5861089, 4.4622434]	
		\widehat{r}_N	[0.2330815, 0.3825372]	[0.5090559, 0.522526]	[0.3452902, 0.4250597]	[0.3715099, 0.4821055]	[11.25986, 14.02245]	
		\widehat{u}_N	[0.01730916, 0.02175581]	[0.2699777, 0.2851786]	[0.1334959, 0.1483957]	[0.1141795, 0.1234791]	[22.07370, 27.90290]	
200	Mean	\widehat{c}_N	[0.02293709, 0.05377072]	[0.007258989, 0.07996798]	[0.005035421, 0.01629725]	[0.02867704, 0.02388901]	[3.5845137, 4.4592981]	
		\widehat{r}_N	[3.178766, 4.3341579]	[3.2757924, 4.5264064]	[3.1961086, 4.4394571]	[3.2328265, 4.469106]	[14.23228, 18.11899]	
		\widehat{u}_N	[1.5009392485, 1.90880226]	[1.3323917, 1.6457617]	[1.41553979, 1.7529745]	[1.42216229, 1.7729688]	[-20.53375, -26.14192]	
	MSE	\widehat{c}_N	[4.01770083, 4.5264064]	[3.95167704, 4.98833161]	[3.97905509, 5.02742585]	[4.00374171, 5.05069556]	[0.4011279, 0.5302202]	
		\widehat{r}_N	[1.469628, 3.0763090]	[3.5873899, 7.0042411]	[2.1473035, 4.6317177]	[2.0778749, 4.417308]	[129.94555, 207.95695]	
		\widehat{u}_N	[0.1430850599, 0.28597103]	[0.4365696, 0.8751362]	[0.22788066, 0.4815695]	[0.22701091, 0.4589775]	[493.35856, 804.27716]	

RMSE	\hat{c}_N	[0.29702909, 0.4556755]	[0.58842419, 0.87715491]	[0.39471441, 0.61731889]	[0.373341717, 0.58668344]	[12.9606399, 20.0024963]	
	\hat{r}_N	[1.4653681, 1.7539410]	[1.8940406, 2.6465527]	[1.4653681, 2.1521426]	[1.4414836, 2.101739]	[11.39937, 14.42071]	
	\hat{u}_N	[0.3782658588, 0.53476259]	[0.6607341, 0.9354871]	[0.47736848, 0.6939521]	[0.47645662, 0.6774788]	[22.21168, 28.35978]	
	\hat{c}_N	[0.54500375, 0.6750374]	[0.76708813, 0.93656549]	[0.62826301, 0.78569644]	[0.611016953, 0.76595264]	[3.6000889, 4.4724150]	
	Bias	\hat{r}_N	[0.178766, 0.3341579]	[0.2757924, 0.5264064]	[0.1961086, 0.4394571]	[0.2328265, 0.469106]	[11.23228, 14.11899]
		\hat{u}_N	[0.0009392485, 0.00880226]	[0.1676083, 0.2542383]	[0.08446021, 0.1470255]	[0.07783771, 0.1270312]	[22.03375, 28.04192]
		\hat{c}_N	[0.01770083, 0.0534642]	[0.04832296, 0.01166839]	[0.02094491, 0.02742585]	[0.003741712, 0.05069556]	[3.5988721, 4.469779]

From table 3 MLE achieved the lowest MSE for most parameters, especially for u_N and c_N , while RTADE performed the worst, with large errors (e.g., the MSE for u_N reached 785.7 for sample size of 50). MLE showed negligible bias (close to zero) for all parameters, while LSE and WLSE had higher but acceptable biases, while RTADE showed a significant bias.

As the sample size increased (from 50 to 200), the accuracy of all methods improved (MSE and RMSE decreased), but the bias decreased significantly, especially for MLE and WLSE. MLE decreased from 0.99 at N=50 to 0.16 at N=200.

Based on the results presented in the table, MLE outperformed the best at estimating parameters with minimal error and bias, and increasing the sample size improved overall accuracy, RTADE performed very poorly, indicating its poor suitability for this model.

Applications on Neutrosophic Data (Time of Failure)

The application side provides a basis for demonstrating the range of the quality, efficacy, and flexibility of NMW-E distribution in practical applications. Time of failure [20] is used to indicate authentic neutrosophic data in this section. Before the analytical procedure starts, the data verified to achieve the neutrosophic characteristics represented by meeting the criterion $T + I + F = 1$. The values must fall inside the interval [0,1], which distinguishes this condition the probability requirement. What distinguishes the neutrosophic logic in table 4 is as follows:

Table 4. Data used, Truth, False, indeterminacy values and verification condition

No.	intervals	Truth (T)	Falsity (F)	Indeterminacy (I)	Sum (T+F+I)	Satisfy neutrosophic condition or not
1	[0.001,0.06]	0.0305	-0.059	1.0285	1	yes
2	[0.011,0.15]	0.0805	-0.139	1.0585	1	yes
3	[0.020,0.25]	0.1350	-0.230	1.0950	1	yes
4	[0.032,0.37]	0.2010	-0.338	1.1370	1	yes
5	[0.071,0.75]	0.4105	-0.679	1.2685	1	yes
6	[0.075,0.81]	0.4425	-0.735	1.2925	1	yes
7	[1.20,1.30]	1.2500	-0.100	-0.1500	1	yes
8	[1.37,1.45]	1.4100	-0.080	-0.3300	1	yes
9	[1.50,1.55]	1.5250	-0.050	-0.4750	1	yes
10	[1.77,1.82]	1.7950	-0.050	-0.7450	1	yes
11	[1.09,1.85]	1.4700	-0.760	0.2900	1	yes
12	[1.91,1.99]	1.9500	-0.080	-0.8700	1	yes
13	[2.35,2.43]	2.3900	-0.080	-1.3100	1	yes
14	[2.39,2.43]	2.4100	-0.040	-1.3700	1	yes
15	[2.85,2.94]	2.8950	-0.090	-1.8050	1	yes
16	[2.96,3.01]	2.9850	-0.050	-1.9350	1	yes
17	[3.10,3.18]	3.1400	-0.080	-2.0600	1	yes
18	[3.15,3.20]	3.1750	-0.050	-2.1250	1	yes
19	[4.67,4.75]	4.7100	-0.080	-3.6300	1	yes
20	[5.00,5.15]	5.0750	-0.150	-3.9250	1	yes
Mean		1.874	-0.196	-0.678	X	
Sd-values		1.485825	0.238933	1.5968068		
Max-values		5.0750	-0.0400	1.2925		
Min-values		0.0305	-0.7600	-3.9250		

The neutrosophic components (T, I, F) for the failure-time data in Table 4 were derived using a practical engineering approach to capture uncertainty in real-world measurements as follows:

1. Source of Indeterminacy in Failure-Time Data.
2. For each observed failure-time interval $[X_L, X_U]$ in Table 4: Truth (T): Represents the confirmed likelihood of failure. Calculated as the normalized mean of expert assessments or historical failure probabilities for the interval. Indeterminacy (I): Captures uncertainty due to incomplete knowledge or measurement limits. Derived as: $I = \left(\frac{W}{M}\right) \times S$, where W = Interval Width (Reflects precision), M = Max Observed Time, and S = Scaling Factor or Adjusted to ensure $T + I + F \leq 1$ (neutrosophic condition). Falsity (F): Represents confidence in non-failure within the interval which calculated as $F = -(\text{Measurement Errorr})$
3. Validation of Neutrosophic Conditions: $T+I+F=1$ (as shown in Table 4) ensures adherence to neutrosophic set theory.

The above table shows that each value meets the criteria, proving that the data complies with the properties of neutrosophic logic. Furthermore, a change in actual values is shown by T values progressive reduction over time. the table faithfully represents real facts by applying neutrosophic logic. The values demonstrate the systems potential adaptability in representing T, F , and I . The results validate that neutrosophic logic may be applied to the processing of complex and unclear data.

The following figures shows the data used, the type of analysis, and the analysis's components.

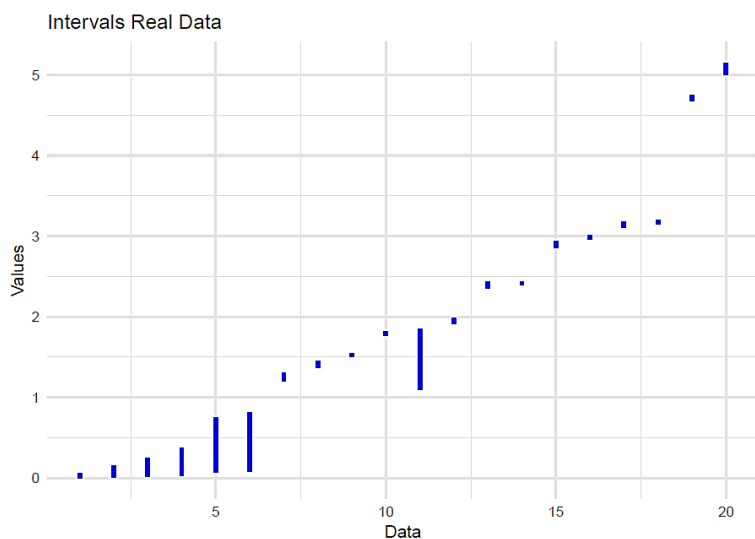


Figure 6. Plot of the intervals for the data used

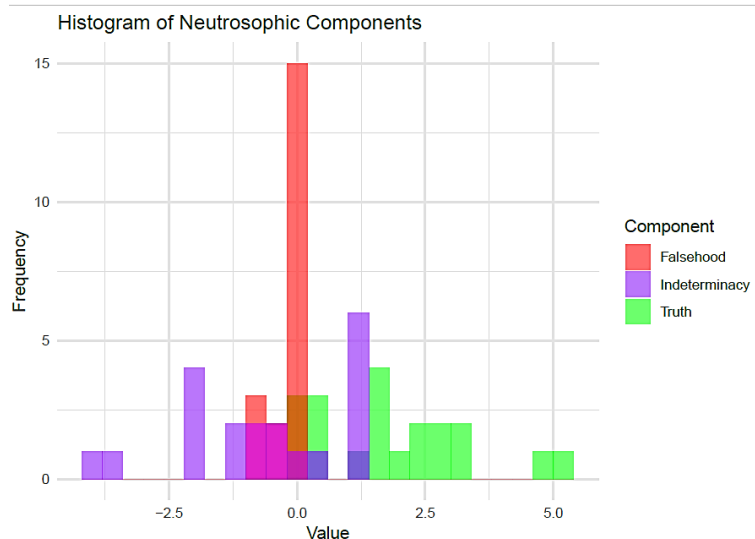


Figure 7. Histogram of Neutrosophic Components

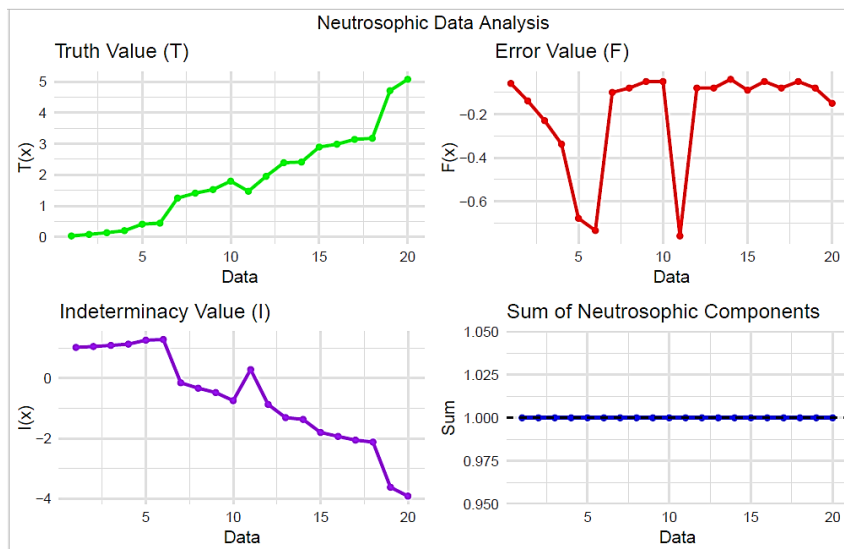


Figure 8. Neurosophic parts and sum of Neurosophic Components

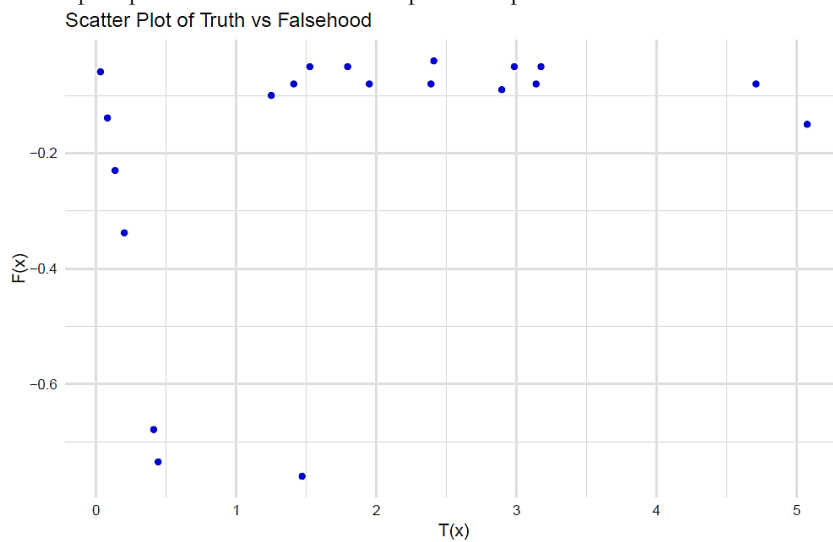


Figure 9. Scatter plot of Truth vs Falsehood

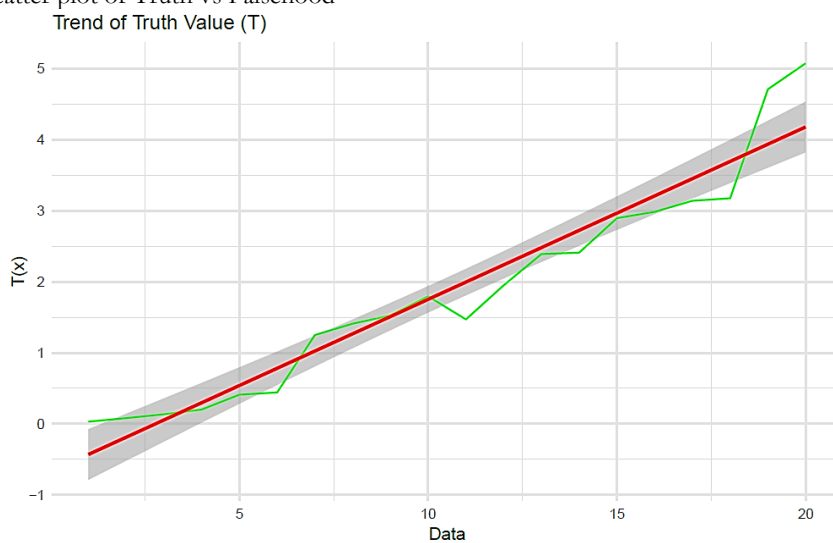


Figure 10. Trend plot of Truth value

The following six potential neurosophic distributions are constructed with the results of NMW-E distribution:

- Neurosophic Odd Lomax Exponential (NOL-E) distribution.
- Neurosophic Kumaraswamy Exponential (NK-E) distribution.
- Neurosophic Exponented Generalized Exponential (NEG-E) distribution.

- Neutrosophic Log-Gamma Exponential (NLG-E) distribution.
- Neutrosophic Beta Exponential (NB-E) distribution.
- Neutrosophic Exponential (N-E) distribution.

For this comparison, four information criteria: AIC, CAIC, HQIC, and BIC, as well as statistical measure like p-value, Anderson-Darling (A), Cramér-von Mises (W), and Kolmogorov-Smirnov (KS) were employed. Table 5 presents the findings of distribution's criteria, table 6 shows the statistical measure values, and table 7 shows estimated parameters in MLE.

Table 5. results of the criteria for the distributions

Dist.	-log	AIC	CAIC	BIC	HQIC
NMW-E	[22.95348, 31.89381]	[51.90695, 69.78762]	[53.40695, 71.28762]	[54.89415, 72.77482]	[52.49009, 70.37076]
NOL-E	[26.05048, 33.21667]	[58.10097, 72.43334]	[59.60097, 73.93334]	[61.08816, 75.42054]	[58.6841, 73.01647]
NK-E	[26.54576, 32.99322]	[59.09152, 71.98644]	[60.59152, 73.48644]	[62.07872, 74.97364]	[59.67466, 72.56958]
NEG-E	[27.69079, 33.27841]	[61.38158, 72.55682]	[62.88158, 74.05682]	[64.36877, 75.54402]	[61.96471, 73.13995]
NLG-E	[29.13772, 32.87706]	[64.27545, 71.75412]	[65.77545, 73.25412]	[67.26264, 74.74131]	[64.85858, 72.33725]
NB-E	[27.80943, 33.39078]	[61.61887, 72.78155]	[63.11887, 74.28155]	[64.60607, 75.76875]	[62.202, 73.36469]
N-E	[31.48727, 78.06966]	[64.97455, 158.1393]	[65.19677, 158.3615]	[65.97028, 159.135]	[65.16892, 158.3337]

Table 6. value of the statistical measures

Dist.	W	A	K-S	p-value
NMW-E	[0.04576082, 0.0321864]	[0.3341181, 0.2234293]	[0.1263261, 0.1127663]	[0.8681040, 0.9611240]
NOL-E	[0.1488689, 0.075885]	[0.8319927, 0.4466335]	[0.2095843, 0.1456056]	[0.2996868, 0.7902015]
NK-E	[0.1608949, 0.06677583]	[0.9015652, 0.3966302]	[0.2111355, 0.1272418]	[0.2916513, 0.9024336]
NEG-E	[0.2206942, 0.07780621]	[1.171433, 0.4574158]	[0.2606936, 0.1503307]	[0.1093530, 0.7567144]
NLG-E	[0.2620839, 0.06182323]	[1.377363, 0.3691157]	[0.2574079, 0.1196168]	[0.1174837, 0.9371271]
NB-E	[0.224453, 0.08124692]	[1.190899, 0.4769215]	[0.2610279, 0.1523129]	[0.1085520, 0.7423199]
N-E	[0.2220572, 0.4481655]	[1.180706, 2.456589]	[0.2586495, 0.7039245]	[0.1143552, 4.933386 × 10 ⁻⁹]

Table 7. Estimator value interval for parameters by MLE

Dist.	$\hat{\mu}_N$	$\hat{\sigma}_N$	\hat{c}_N
NMW-E	[0.3014412, 0.3610247]	[0.1612506, 0.4600951]	[3.2192589, 1.0134697]
NOL-E	[0.3402548, 1.2854050]	[0.0989092, 4.7513380]	[4.6372997, 0.1333090]
NK-E	[0.2800673, 1.2620136]	[0.1677715, 12.6776875]	[2.7624720, 0.0663569]
NEG-E	[0.6527687, 0.5960127]	[0.5178731, 1.2673610]	[0.5569602, 0.9823615]
NLG-E	[0.6691136, 1.2614760]	[0.5113513, 3.3182570]	[0.3456222, 1.5754780]
NB-E	[34.5875008, 39.6218952]	0.5173902, 1.2786216]	[0.0105736, 0.0151257]
N-E	---	---	[0.5630631, 0.0568178]

From table 5, NMW-E has the lowest values for all criteria, indicating that it is the best fit among all the other distribution, NOL-E and NK-E are close to it, but with slightly higher values. NEG-E, NLG-E, and NB-E have worse values, N-E (the simple exponential neutrosophic distribution) performs very poorly, especially since its AIC and BIC values are very high, indicating that it is not a good fit.

From table 6, NMW-E achieved the highest p-values (between 0.868 and 0.961), which is very excellent, indicating its fit to data. NOL-E and NK-E had acceptable p-values, indicating poor fit, while N-E clearly performed very poorly (p-values well below 0.05).

From table 6, NMW-E has narrow and consistent estimation intervals, indicating model stability. NOL-E and NK-E have much wider estimation intervals, which implies greater instability or dispersion in data.

For visual verification, the fitted Npdf is plotted with a histogram of data used for the NMW-E (best) distribution, and the empirical fitted NMW-E NCDF is plotted.

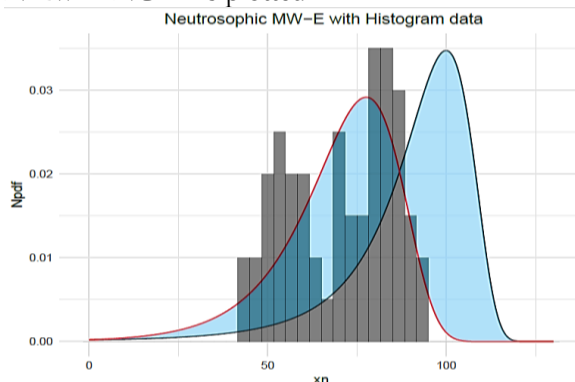


Figure 11. NMW-E with histogram data

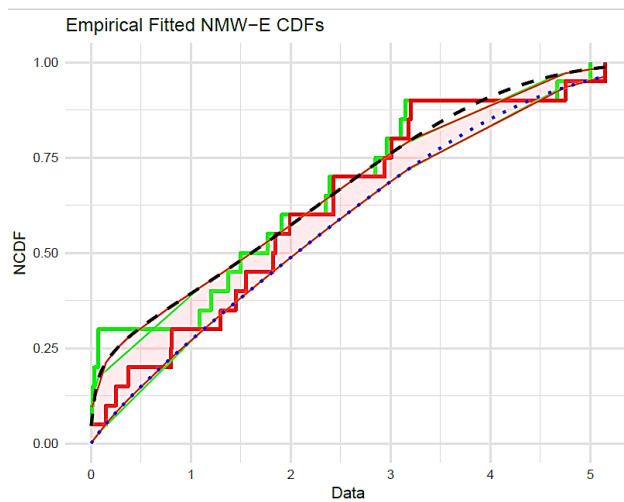


Figure 12. empirical fitted NMW-E CDF

In electronics reliability analysis (component failure time), small samples are common due to the high cost or long time required to collect data. Small samples ($n=10-30$) are often used due to the infrequency of failures in accelerated testing. For the statistical analysis, KS and A-D criteria were used with high p -values (0.86–0.96), demonstrating a good fit of the data to the model even with a small sample size. To compensate for the limited real sample size, Monte Carlo simulations (1000 samples) were performed with different sample sizes ($n=50, 100, 150, 200$) as shown in Table 3. The results showed stable parameters and decreased mean deviation (Bias) and mean standard error (RMSE) with increasing sample size, especially when using MLE.

CONCLUSIONS

A new distribution family, called Neutrosophic Modified Weibull-G (NMW-G), was constructed combining the Modified Weibull distribution with Neutrosophic logic, with a special model, NMW-E. The new model efficiently addresses the problem of ambiguous and missing data through a flexible mathematical structure that includes: a NCDF, Npdf, survival and hazard functions, and expansions using Taylor series and binomials. Through Monte Carlo simulations with five estimation methods, the estimation results showed that MLE method is most efficient, with high estimation accuracy and low bias, especially as the sample size increases. Other methods, such as RTADE, performed worse, exhibiting very high bias and estimation errors. In a practical application of failure time data of 20 electronic components, the Neutrosophic logic condition was verified for all values. The NMW-E distribution clearly outperformed the other competing distributions (NOL-E, NK-E, NEG-E, NLG-E, NB-E, N-E). Based on the results of statistical criteria and goodness-of-fit tests, the NMW-E distribution achieved the lowest values of the selection criteria and the highest p -values. The NMW-E distribution has proven its high flexibility and its ability to represent realistic data with uncertainty better than classical models.

Funding Statement

This work was supported and funded by the Deanship of Scientific Research at Imam Mohammad Ibn Saud Islamic University (IMSIU) (grant number IMSIU-DDRSP2501).

REFERENCE

- J. Farrukh, H. Bakouch and A. N. M., "A truncated general-G class of distributions with application to truncated Burr-G family," *REVSTAT-Statistical Journal*, pp. 513-530, 4 19 2021.
- A. L. Solomon Sarpong and S. Nasiru, "Odd Chen-G family of distributions," *Annals of Data Science*, pp. 369-391, 2 9 2022.
- I. A. Sadiq, S. I. S. Doguwa, A. Yahaya and A. Usman, "Development of New Generalized Odd Fréchet-Exponentiated-G Family of Distribution," *A periodical of the Faculty of Natural and Applied Sciences, UMYU, Katsina*, p. 169 – 178, 4 2 2023.
- J. N. Al Abbasi, I. A. Resen, A. M. Abdulwahab, P. E. Oguntunde, H. Al-Mofleh and M. A. Khaleel, "The right truncated Xgamma-G family of distributions: Statistical properties and applications," *AIP Conference Proceedings*, 1 2834 2023.

- F. Smarandache, "A unifying field in logics. neutrosophy: Neutrosophic probability, set and logic," Rehoboth, 1999.
- F. Smarandache, "A geometric interpretation of the neutrosophic set-A generalization of the intuitionistic fuzzy set," arXiv preprint math, p. 0404520, 2004.
- M. M. Alanaz, M. Y. Mustafa and Z. Y. Algamal, "Neutrosophic Lindley distribution with application for Alloying Metal Melting Point," *International Journal of Neutrosophic Science*, pp. 65-71, 4 21 2023.
- K. Zahid , M. M. A. Almazah , O. H. Odhah and H. M. Alshanbari, "Generalized pareto model: properties and applications in neutrosophic data modeling. *Mathematical Problems in Engineering*," *Mathematical Problems in Engineering*, p. 3686968, 1 2022.
- M. M. Alanaz and Z. Y. Algamal, "Neutrosophic exponentiated inverse Rayleigh distribution: Properties and Applications," *International Journal of Neutrosophic Science*, pp. 36-43, 4 21 2023.
- O. E. Al-Saqal, Z. A. Hadied and Z. Y. Algamal, "Modeling bladder cancer survival function based on neutrosophic inverse Gompertz distribution," *International Journal of Neutrosophic Science*, pp. 75-5, 1 25 2025.
- Z. Y. Algama, N. N. Alobaidi, A. A. Hamad, M. M. Alanaz and M. Y. Mustafa, "Neutrosophic Beta-Lindley distribution: Mathematical properties and modeling bladder cancer data," *International Journal of Neutrosophic Science*, pp. 186-194, 2 23 2024.
- Z. Khan, M. M. A. Almazah, O. H. Odhah and H. M. Alshanbari, "Generalized Pareto Model: Properties and Applications in Neutrosophic Data Modeling," *Mathematical Problems in Engineering*, p. 3686968, 1 2022.
- A. Alzaatreh, C. Lee and F. Famoye, "A new method for generating families of continuous distributions," *Metron*, p. 63–79, 71 2013.
- S. Rezaei, A. K. Marvasty, S. Nadarajah and M. Alizadeh, "A new exponentiated class of distributions: Properties and applications," *Communications in Statistics-Theory and Methods*, pp. 6054-6073, 12 46 2017.
- H. M. Almongy, E. M. Almetwally, H. M. Aljohani, A. S. Alghamdi and E. H. Hafez, "A new extended Rayleigh distribution with applications of COVID-19 data," *Results in Physics*, p. 104012, 23 2021.
- Z. Shah, D. M. Khan, Z. Khan, N. Faiz, S. Hussain, A. Anwar, T. Ahmad and K.-I. Kim, "A new generalized logarithmic–X family of distributions with biomedical data analysis," *Applied Sciences*, p. 3668, 6 13 2023.
- Y. Wang, Z. Feng and A. Zahra, "A new logarithmic family of distributions: Properties and applications," *CMC-Comput. Mater. Contin*, p. 919–929, 66 2021.
- S. Naz, L. A. Al-Essa, H. S. Bakouch and C. Chesneau, "A transmuted modified power-generated family of distributions with practice on submodels in insurance and reliability," *Symmetry* , p. 1458, 7 15 2023.
- O. A. Bello, S. I. Doguwa, A. Yahaya and H. M. Jibril, "A type I half Logistic exponentiated-G family of distributions: Properties and application," *Communication in Physical Sciences*, pp. 147-163, 3 7 2021.
- L. A. Al-Essa, J. Farrukh, S. Shakaiba, K. Sadaf, A. Qamer, A. Rehan and M. Aslam, "Properties and Applications of Neutrosophic Burr XII Distribution," *International Journal of Computational Intelligence Systems*, p. 10, 1 18 2025.